The role of final-state interaction modeling in neutrino energy reconstruction and oscillation measurements

Y. Liu,[1,*] L. Munteanu,[2,†] and S. Dolan[2,‡]

[1] University of Chicago, Chicago, IL 60637, USA

[2] European Organization for Nuclear Research (CERN), 1211 Geneva 23, Switzerland

(Dated: November 7, 2025)

Next-generation long-baseline neutrino oscillation experiments promise to provide dramatically improved measurements of PMNS neutrino oscillation parameters, including measurements of charge-parity violation in the lepton sector, in addition to searches for new physics. Achieving such precise measurements requires inferring neutrino oscillation probabilities over a wide neutrino energy range, which demands the most accurate neutrino energy reconstruction through precise measurements of all visible final-state particles produced in neutrino interactions. However, any reconstruction will inevitably miss a significant fraction of energy when it is, for example, carried away by neutrons, the nuclear remnant or unidentified charged pions. The size of the subsequent neutrino energy reconstruction bias is affected by many aspects of neutrino interaction physics, but the poorly understood re-interactions of struck hadrons within the nuclear medium, final-state interactions (FSI), are especially important. In this work, we assess how variations of FSI modeling affect neutrino energy reconstruction. As a case study, we use the neutrino flux and baseline of the upcoming DUNE experiment to illustrate that FSI model variations, in the absence of robust near-detector constraints, have the potential to be degenerate with variations of neutrino oscillation parameters at the level of projected precision for future measurements. The results highlight the need for further development of sophisticated FSI models, alongside capable near detectors at next-generation experiments to constrain them.

Introduction — Long-baseline (LBL) neutrino oscillation experiments are essential for advancing our understanding of neutrino properties, including critical measurements of mass-squared differences and mixing angles. Future experiments, such as the Deep Underground Neutrino Experiment (DUNE) [1] and Hyper-Kamiokande (Hyper-K) [2, 3], aim to push the frontier by precisely measuring the parameters that govern neutrino oscillations, searching for charge-parity (CP) violation in the lepton sector, resolving the neutrino mass ordering, and searching for signatures of new physics [3, 4].

A vital component of these measurements is the precise reconstruction of the incoming neutrino energy from the products of charged-current neutrino interactions with the nuclear targets within detectors, alongside an associated accurate modeling of the true-to-reconstructed neutrino energy response function [5]. This is particularly important for experiments like DUNE that are designed with a broad-band neutrino beam and will infer oscillation probabilities over a wide energy range. The core technology of the DUNE detectors is the liquid argon time projection chamber (LArTPC), which can provide a detailed reconstruction of neutrino interaction products following neutrino interactions with argon nuclei [1]. The reconstruction of the incident neutrino energy relies on summing the energy of the interaction products. Since neutral particles are largely invisible in a LArTPC, the accuracy of neutrino energy reconstruction depends on the modeling of the constituents of the hadronic final state. In this context, several processes warrant careful investigation. Of particular importance are final-state interactions (FSI), where hadrons produced in the initial neutrino interaction undergo further scattering inside the nucleus before exiting, thereby altering observable particle multiplicities and kinematics [5, 6].

FSI can alter the kinematics and even change the type of particles that can be detected in the final state of neutrino interactions, leading to biases and uncertainties in the inferred neutrino energy [5]. These biases pose concerns as they can obscure oscillation effects, potentially causing degeneracies with oscillation parameters. Furthermore, there are large uncertainties associated with the models that describe FSI processes [6].

In this work, we use simulations of neutrino interactions with different FSI models with the DUNE neutrino flux [1, 7] and baseline (1300 km) as a case study to assess how different FSI models affect reconstructed neutrino energies and the resulting energy spectra. We then investigate how these distortions compare to the variations in oscillation parameters at the level of precision that future LBL experiments aim to measure [3, 8]. Through this study, we highlight the potential for plausible variations of FSI modeling to be degenerate with variations of neutrino oscillation parameters, thereby emphasizing the need for precise modeling of FSI to achieve the experiments' ambitious goals.

Method and models — The goal of the analysis is to evaluate how the expected reconstructed spectrum of neutrino energies at the DUNE far detector baseline varies with alterations to FSI modeling and how this compares to the variations of neutrino oscillation parameters.

Charged-current neutrino interactions with argon are generated using the `GENIE v3.04.00` neutrino event generator [9, 10] using a fixed neutrino-nucleus interaction model apart from alterations to the simulation of FSI. Electron and muon neutrino and antineutrino interactions are generated using fluxes expected at the DUNE near detector (i.e. before oscillations occur) [1, 7] and then weighted to apply oscillations using the `Prob3++` software package [11, 12]. The baseline set of neutrino oscillation parameters considered are $\sin^2\theta_{12} = 0.307$, $\sin^2\theta_{13} = 0.0219$, $\sin^2\theta_{23} = 0.558$, $\Delta m^2_{21} = 7.53\times10^{-5}$ eV^2, $\Delta m^2_{32} = 2.455\times10^{-3}$ eV^2, taken from Ref. [13], $\delta_{\rm CP} = 0$ by default and a normal neutrino mass ordering. Matter effects are treated using the default implementation within `Prob3++` [11, 12].

The baseline interaction model uses the `G18_10a_00_000 GENIE` configuration [14], employing a local Fermi-gas nuclear ground state, the Valencia group's model for CCQE and 2p2h interactions [15–17], and the Berger-Seghal resonance and coherent pion production models [18, 19]. Higher energy transfer interactions are modeled using the GRV98 PDFs [20] with Bodek-Yang corrections [21] and hadronization from either PYTHIA [22, 23] (at high invariant masses, W, above 3.0 GeV/c^2) or the custom AGKY model [24] (for $W < 2.3$ GeV/c^2), with an interpolation between the two routines at intermediate values of W [25].

FSI are modeled using one of four different models available within GENIE: the default hA2018 model, the hN2018 model (for a description of these two models see [14]), the Liege Intranuclear Cascade model (INCL) [26][1], or the GEANT4 Bertini Cascade model (G4BC) [27]. For the purpose of this focused study, all other aspects of the interaction model are kept the same as the baseline. More details and comparisons of these FSI models are available in Refs. [6, 28]. For the purposes of this work, it is sufficient to note that the hA2018 and hN2018 models are representative of those widely used as inputs to current neutrino oscillation and cross-section measurements whilst INCL and G4BC represent more sophisticated simulations that have been only recently incorporated into neutrino event generators. In the absence of a comprehensive parameterisation of systematic uncertainties on FSI models, the span of these models provides a reasonable means of estimating a minimal plausible variation. For reference, a simulation with no FSI is also considered.

In this work, it is assumed that a reasonable proxy for reconstructed neutrino energy ($E_\nu^{\rm rec}$) can be defined as:

$$E_\nu^{\rm rec} = E_\ell + \sum_{i=p} T_i + \sum_{i=\pi,K,\gamma} E_i. \qquad (1)$$

This is the sum of the lepton energy (E_ℓ), the kinetic energies (T) of all final-state protons, and the total energy (E) of all pions, kaons (charged or neutral) and photons. No selection effect or energy threshold is applied. We define the relative neutrino energy bias as $(E_\nu^{\rm rec} - E_\nu^{\rm true})/E_\nu^{\rm true}$, which is primarily driven by the amount of energy carried away by neutrons. Ref. [29] provides a discussion of this reconstructed neutrino energy metric and how it compares with others.

Using Equation 1 is largely equivalent to assuming that a neutrino detector acts as a perfect calorimeter whilst successfully identifying the multiplicity of charged pions whose mass energy (which is lost largely to neutrinos from the pion decay) is added to the calorimetric sum. This is broadly illustrative of what might be expected from DUNE's LAr TPCs, which can use a combination of tracking and calorimetry to achieve this high precision for neutrino energy reconstruction. However, the relationship between this proxy and the true neutrino energy depends on the modeling of effects which modify the visible energy in the detector, like FSI. It should be noted that Equation 1 is not applicable to the case of water Cherenkov detectors, which are used for Hyper-K, as these are not sensitive to most hadrons below Cherenkov threshold.

Figure 1 shows the simulated distribution of neutrino energy bias for muon neutrino and antineutrino charged-current interactions, using the DUNE neutrino and antineutrino beam-mode fluxes respectively before oscillations occur, for a variety of different FSI models, including one simulation without FSI. It is apparent that FSI has a significant impact on neutrino energy reconstruction and that different FSI models lead to significantly different energy bias profiles. Moreover, we note that FSI, and the sources of invisible energy it introduces, has a different impact on the energy reconstruction of neutrinos with respect to antineutrinos. Whilst neutrino interactions occur primarily with neutrons in the nucleus, and as a result often produce protons or other charged particles in the absence of FSI, antineutrinos reverse this behavior and naturally produce more neutrons in the final state. This can be observed in the much broader distribution of the relative bias in the antineutrino case. As a reference point, for the models considered, the fraction of events with a bias larger than 10% is of order 40% for neutrinos and 50% for antineutrinos.

Variations to the reconstructed neutrino energy spectra for muon (anti)neutrino disappearance and electron (anti)neutrino appearance channels from alterations of FSI modeling are compared to variations of neutrino oscillation parameters. The latter are chosen to be comparable to next-generation experiments' long-term projected precision [3, 8]. For reference, these are also compared to expected statistical uncertainties on the measured reconstructed neutrino energy spectra from a projected exposure of ten years of the DUNE experiment (corresponding to 624 kt-MW-years, equally split between beam operation in neutrino and antineutrino run-

[1] The current GENIE implementation of INCL is known not to replicate all physics of the original code. Work is ongoing to improve the implementation.

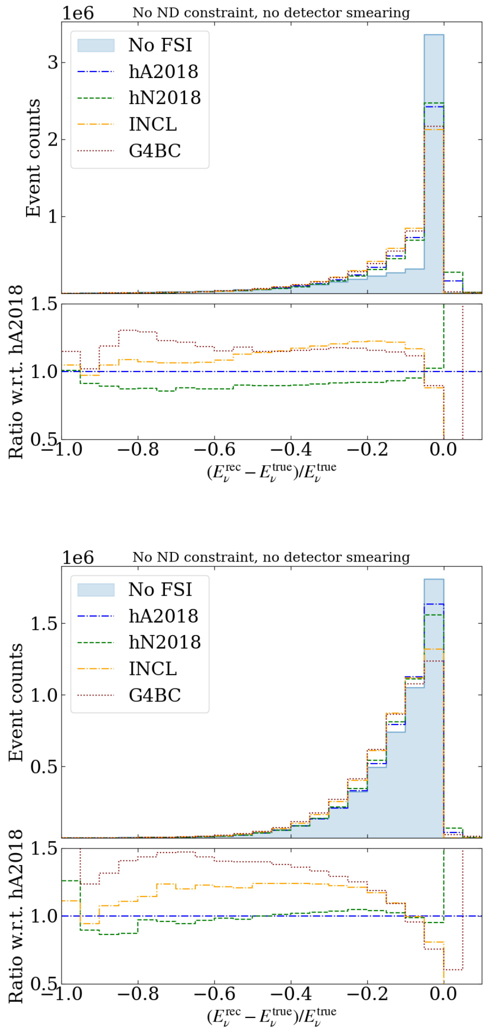

Fig. 1: The simulated distribution of neutrino energy bias for muon neutrino (top) and antineutrino (bottom) charged-current interactions, using the DUNE neutrino and antineutrino beam-mode fluxes respectively before oscillations occur, for a variety of different FSI models. Each distribution is generated using 5 million charged-current events. The blue shaded histogram assumes no FSI, while the other histograms correspond to the four FSI models. The expression for $E_\nu^{\rm rec}$ is given in Equation 1 and E_ν corresponds to the true neutrino energy. The bottom panel shows the ratios of different FSI models with respect to the hA2018 baseline model.

ning modes [8][2]). In these studies, we consider that there is no background contribution from wrong-sign or wrong-flavor neutrino candidates or neutral-current interactions.

Results — We first examine the effect of FSI modeling on reconstructed energy spectra relevant to ν_μ disappearance analyses, in both neutrino and antineutrino beam modes. Figure 2 shows the reconstructed oscillated spectra using different FSI models, overlaid with $\pm 0.4\%$ variations of Δm^2_{32}. As indicated in the bottom panel in each sub-figure, the shifts induced by FSI variations are comparable in size to the simulated variations of Δm^2_{32}, and reproduce characteristic features of oscillation parameter variations near the first oscillation maximum (i.e. a shift in the energy spectrum). Additional figures comparing the FSI effects with corresponding variations in $\sin^2\theta_{23}$ are provided in the Supplemental Material.

A similar analysis is performed for the ν_e appearance channel, which drives the sensitivity to identification of CP violation (CPV) and the precise measurement of the CP-violating phase $\delta_{\rm CP}$. Figure 3 shows the reconstructed ν_e and $\bar{\nu}_e$ spectra under the CP conservation ($\delta_{\rm CP} = 0$) and maximal CPV ($|\delta_{\rm CP}| = \pi/2$) hypotheses. When referring to maximal CPV across the study, we choose to only consider the case where $\delta_{\rm CP}$ is -$\pi/2$, which is closest to the current knowledge [13]. Since sensitivity to measuring $\delta_{\rm CP}$ depends on its value, this is shown alongside an error band of $\pm\pi/10$ or $\pm\pi/20$ for the CP-conserving and CP-violating cases respectively, approximately corresponding to the projected precision reported in Refs. [3, 8]. Across all four panels, the variations from FSI modeling are comparable to, or exceed, the size of spectral differences induced by varying $\delta_{\rm CP}$. However, as can also be seen by comparing the integrated event rate of CP-conserving case to the CP-violating case, the observation of CPV in the ν_e appearance channel is clearly robust against considered FSI modeling variations if CPV is maximal. Whilst not shown here, we also studied the sensitivities to the θ_{23} octant determination and the neutrino mass ordering, concluding that the considered FSI modeling uncertainty has minimal impact on these measurements (for the oscillation parameters considered within this work).

Discussion and outlook — It is clear from Figure 1 that FSI changes the magnitude and shape of the bias in the reconstruction of neutrino energy. For example, the amount of events with more than 10% relative bias varies by about 30% (20%) between (anti)neutrino model predictions under variations of FSI. Whilst not explicitly shown here (as Figure 1 is integrated over a broad-band flux), the characteristics of the bias also change as a function of neutrino energy itself.

The FSI-induced modification in reconstructed neutrino energy bias manifests as shifts in the measured neutrino energy spectra. Notably, this affects the *measured* position of the first oscillation maximum (i.e. minimum muon neutrino survival probability), whose position as a function of *true* neutrino energy is determined by the

[2] The total signal statistics have been obtained by scaling the signal statistics reported in [8] by the ratio between 336 kt-MW-years (7 years) and 624 kt-MW-years (10 years) exposures.

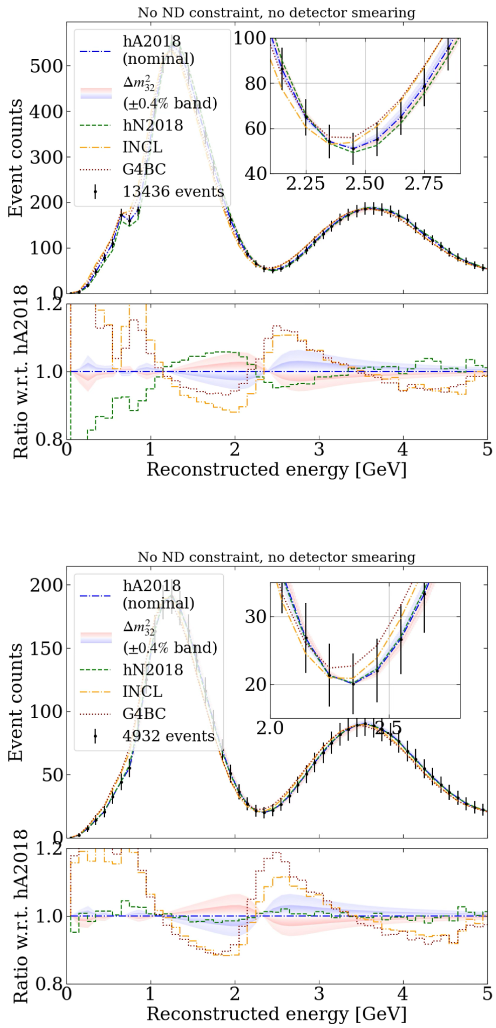

Fig. 2: Comparison of the simulated ν_μ reconstructed energy spectra and an oscillated DUNE experiment flux using different FSI models, to variations of Δm^2_{32}. This is simulated for neutrino (top) and antineutrino (bottom) beam modes. In each sub-figure, reconstructed energy spectra under different FSI models are shown as histograms and $\pm 0.4\%$ Δm^2_{32} variations are shown with shaded blue (+) and red (-) bands centered on the hA2018 baseline. The error bars are broadly indicative of the DUNE experiment's statistical uncertainty with 10 years of operation. The inset provides a zoomed-in view of the first oscillation maximum. The lower panel displays ratios of FSI model and Δm^2_{32} variations relative to the hA2018 baseline. In the lower panel, the bands show 1-σ (inner) and 2-σ (outer) variations to Δm^2_{32}.

value of Δm^2_{32}. In Figure 2, the size of the FSI model spread around the measured first oscillation maximum is larger than that of a 0.4% shift in Δm^2_{32}. This highlights the risk of a degeneracy between FSI effects and variations of Δm^2_{32} in the data of far detectors for LBL experiments. It is worth noting that for both the neutrino and antineutrinos cases, the most significant differences with respect to the baseline hA2018 model are exhibited by the sophisticated G4BC and INCL models.

In the case of true maximal CPV, our analysis indicates that the impact of FSI modeling is not likely to be decisive in the search for CPV since the majority of this sensitivity comes directly from the relative amount of observed electron neutrinos and antineutrinos rather than shape alterations in the reconstructed neutrino energy spectra. However, the situation is different for precision measurements of $\delta_{\rm CP}$. In this case, the measurement can be influenced by effects that alter the shape of the reconstructed electron (anti)neutrino energy spectrum, and the degree of sensitivity depends on the true value of $\delta_{\rm CP}$. As shown in Figure 3, when $\delta_{\rm CP} \sim -\pi/2$, variations in $\delta_{\rm CP}$ primarily manifest as shape changes in the reconstructed energy spectra, whereas for $\delta_{\rm CP} \sim 0$, they appear more as overall rate differences. Since the shape dependence resembles the effects introduced by variations in FSI modeling, we conclude that for precision $\delta_{\rm CP}$ measurements, FSI uncertainties may obscure the result if the true value of $\delta_{\rm CP}$ corresponds to near-maximal CPV.

The results presented in this work offer a qualitative assessment of the impact of FSI, intended to motivate more careful treatment to these effects in view of future oscillation analyses. However, there are a number of limitations to our analysis. First, we simply consider variations between FSI models on reconstructed neutrino energy energy spectrum as a proxy for their potential effect on neutrino oscillation analyses, neglecting the effect they will have on any constraint propagated from a near detector. In the case of DUNE, the near detector is clearly well equipped to constrain plausible variations from FSI modeling [30], but doing so requires a comprehensive parameterisation of FSI, as well as other neutrino interaction uncertainties, to be fitted to the near detector data. Second, we only consider two sets of oscillation parameters. In reality, correlations between oscillation parameters will change the expected sensitivity of the measurements. However, we expect that the qualitative conclusions of the study will not change for other combinations of oscillation parameters within the ranges allowed by current experimental measurements (see, e.g., Ref. [13]). Third, we only examine FSI variations on the size of the expected shape of the oscillated signal, neglecting its potential impact on backgrounds (such as wrong sign, wrong flavor or neutral current interactions). Fourth, in this study we consider the effect of FSI variations on the reconstructed neutrino energy spectrum in isolation of other observables. It is potentially possible to choose an alternative set of far detector observables which could help disambiguate FSI effects from genuine neutrino oscillations (e.g. by using transverse or generalized kinematic imbalance variables [31–

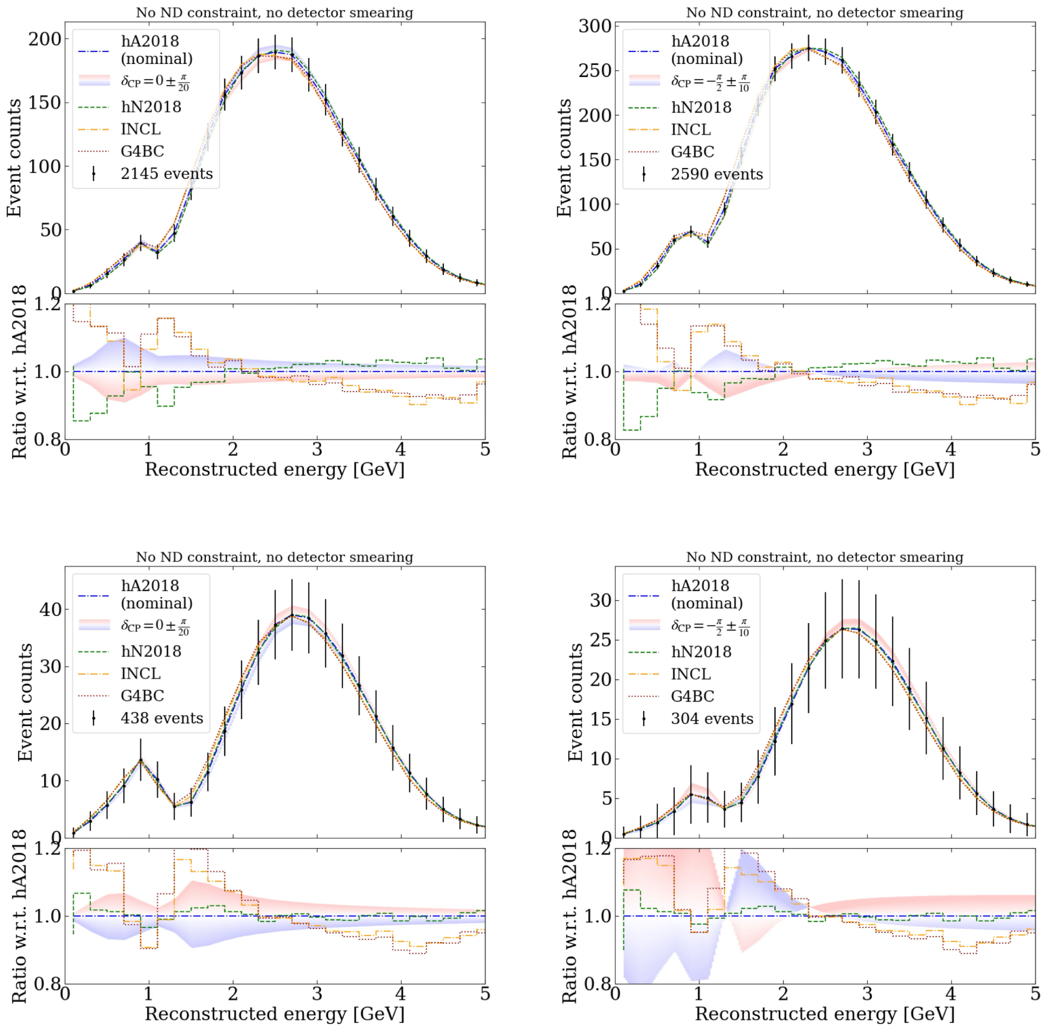

Fig. 3: Comparison of the simulated ν_e reconstructed energy spectra and an oscillated DUNE experiment flux using different FSI models, to variations of Δm^2_{32}. This is simulated for neutrino (top) and antineutrino (bottom) beam modes. The left and right correspond to $\delta_{\mathrm{CP}} = 0$ and $\delta_{\mathrm{CP}} - \pi/2$, respectively. Other figure elements follow the same conventions as described in Figure 2, except that only the 1-σ uncertainty band is shown in the lower panels.

34]). We note that regardless of the choice of observables, their relationship to the true neutrino energy remains a model-depending mapping which in turn must be accompanied by an appropriate uncertainty parameterisation and therefore an improved understanding of FSI. Fifth, we do not account for detector effects or backgrounds to far detector event selections from neutral current interactions, neutrinos of the wrong flavor or sign, and the intrinsic electron neutrino contamination to the DUNE beam. Whilst these backgrounds are small for neutrino analyses ($\lesssim$20% [8]) they can be large for antineutrino samples (up to $\sim$65% [8]). The quantity and shape of the backgrounds will themselves also be impacted by FSI.

This work does not consider potential variation of the reconstructed neutrino energy spectra from sources of uncertainty beyond FSI. Modeling of other nuclear effects, particularly those that can significantly alter the hadronic system (e.g. hadronization), and detector response gives scope for significantly more variation.

Despite the above limitations, our analysis demonstrates the plausible impact that varying FSI alone can have on reconstructed neutrino energy spectra and compares it to oscillation parameter variations, showing scope for significant degeneracy between the two. This suggests that a near detector system, alongside an appropriate uncertainty model, is a crucial tool for mitigating FSI-related systematic uncertainties. In particular, the More Capable Near Detector (MCND) [35] for DUNE Phase II will likely play a critical role in constraining interaction models through its enhanced ability to revolve final-state particles via low particle tracking thresholds. Moreover, the movable DUNE near detector system may be able to leverage the PRISM technique to remove oscillation measurement bias in FSI modeling in exchange for larger uncertainties [30].

Beyond near detector measurements, further progress will require concerted theoretical guidance and experimental efforts to refine FSI models and associated uncertainty parameterisations. As highlighted in Ref. [6], measurements of hadron scattering on argon remain limited, despite their indispensable role in validating FSI models. Modern LArTPC experiments including LArIAT [36] and ProtoDUNE [37, 38] have begun to address this gap by using hadron test beams to measure cross sections for hadron-argon interactions. Several results have been published [39, 40]. Although these measurements currently suffer from large uncertainties, future exclusive or differential cross-section measurements, which could build on work like the differential analyses from the HADES experiment [41, 42], may offer significant discriminating power between different FSI models. A useful set of measurements would be those quantifying the fraction of initial-state hadron energy remaining visible in the final state inside a LArTPC (thereby constraining the shape of Figure 1). As another important experimental input, neutrino or electron scattering data from dedicated cross-section experiments also contribute to constraining FSI within neutrino interactions relevant for DUNE. MicroBooNE [43] has released a broad set of measurements across various channels of neutrino interactions and upcoming results from SBND [44], with their increasing statistics, will further expand on these. While the neutrino beams in these experiments have generally lower energies compared to the DUNE beam, these datasets can be complemented by those from ICARUS [45] and the DUNE:2x2 prototype detector [46], which operate in a higher energy neutrino beam. These neutrino scattering analyses are further complemented by precise electron scattering measurements using a variety of nuclear targets and energies [47]. The high statistics and known incoming electron energy permits the isolation of kinematic phase space to precisely probe FSI (see e.g. Ref. [48]). Additionally, the proposed nuSCOPE experiment at CERN [49] offers event-by-event knowledge of *neutrino* energy, covering the full range of energies of interest to DUNE. Measurements from nuSCOPE would allow an almost direct measurement of the neutrino energy bias shown in Figure 1, thereby eliminating much of the need to rely on poorly-constrained neutrino interaction models to predict expected neutrino energy reconstruction performance.

Whilst the case study shown uses the DUNE flux and baseline, the qualitative conclusions are likely to be broadly applicable to any neutrino oscillation experiment relying on the calorimetric neutrino energy reconstruction implied by Equation 1. Conversely, the conclusions of this study cannot be directly translated to other methods of neutrino energy reconstruction such as those used by Hyper-K. The use of water Cherenkov detectors necessitates a less precise neutrino reconstruction method which primarily relies on inferring the neutrino energy from final-state lepton kinematics under the assumption of a quasi-elastic two-body scatter. FSI effects are still relevant for this method, but intervene mostly through the modeling of pion absorption processes which may contaminate quasi-elastic-like samples [5].

Conclusions — In conclusion, this study demonstrates that FSI modeling uncertainties have the potential to alter reconstructed neutrino energy spectra in ways which are degenerate with variations of neutrino oscillation parameters. The variations in reconstructed energy spectra due to different FSI models are comparable to, or even exceed, the projected precision of next-generation experiments to Δm^2_{32} and $\delta_{\rm CP}$. Whilst this work offers only a qualitative illustration of FSI effects on oscillation measurements, and does not include a simulation of a near detector constraint, among other limitations, it highlights a critical need for improved FSI modeling and comprehensive uncertainty quantification. Future work may focus on conducting dedicated measurements of hadron-argon interactions, understanding disagreement among different FSI models, and implementing robust FSI uncertainty parameterisations to support the ambitious physics goals of next-generation oscillation experiments.

Acknowledgments — YL is supported by the National Science Foundation under Grant No. 2514289, and would like to thank Edward Blucher for fruitful discussions on this study. All authors would like to thank Steven Dytman and Richard Diurba for discussions related to this work. All authors would also like to acknowledge support from the DUNE collaboration, and the suggestions provided by Julia Tena Vidal, Orlando Peres and Vivek Jain during the review of this work.

* Contact e-mail: yinrui@uchicago.edu
† Contact e-mail: laura.munteanu@cern.ch
‡ Contact e-mail: stephen.joseph.dolan@cern.ch

[1] B. Abi *et al.* (DUNE), (2020), arXiv:2002.03005 [hep-ex].
[2] K. Abe *et al.* (Hyper-Kamiokande), (2018), arXiv:1805.04163 [physics.ins-det].
[3] K. Abe *et al.* (Hyper-Kamiokande), (2025), arXiv:2505.15019 [hep-ex].
[4] R. Acciarri *et al.* (DUNE), (2015), arXiv:1512.06148 [physics.ins-det].
[5] L. Alvarez-Ruso *et al.* (NuSTEC), Prog. Part. Nucl. Phys. **100**, 1 (2018), arXiv:1706.03621 [hep-ph].
[6] S. Dytman *et al.*, Phys. Rev. D **104**, 053006 (2021), arXiv:2103.07535 [hep-ph].
[7] `https://home.fnal.gov/~ljf26/DUNEFluxes/OptimizedEngineeredNov2017_offaxis/`, accessed:

2019-08-07.
[8] B. Abi *et al.* (DUNE), Eur. Phys. J. **C80**, 978 (2020), arXiv:2006.16043 [hep-ex].
[9] C. Andreopoulos, C. Barry, S. Dytman, H. Gallagher, T. Golan, R. Hatcher, G. Perdue, and J. Yarba, (2015), arXiv:1510.05494 [hep-ph].
[10] C. Andreopoulos *et al.*, Nucl. Instrum. Meth. A **614**, 87 (2010), arXiv:0905.2517 [hep-ph].
[11] V. D. Barger, K. Whisnant, S. Pakvasa, and R. J. N. Phillips, Phys. Rev. D **22**, 2718 (1980).
[12] `https://github.com/rogerwendell/Prob3plusplus`, accessed: 2025-18-07.
[13] S. Navas *et al.* (Particle Data Group), Phys. Rev. D **110**, 030001 (2024).
[14] J. Tena-Vidal *et al.* (GENIE), Phys. Rev. D **104**, 072009 (2021), arXiv:2104.09179 [hep-ph].
[15] J. Nieves, I. Ruiz Simo, and M. J. Vicente Vacas, Phys. Rev. **C83**, 045501 (2011), arXiv:1102.2777 [hep-ph].
[16] R. Gran, J. Nieves, F. Sanchez, and M. V. Vacas, Physical Review D **88**, 113007 (2013).
[17] J. Schwehr, D. Cherdack, and R. Gran, (2016), arXiv:1601.02038 [hep-ph].
[18] C. Berger and L. M. Sehgal, Phys. Rev. D **76**, 113004 (2007), arXiv:0709.4378 [hep-ph].
[19] C. Berger and L. M. Sehgal, Phys. Rev. D **77**, 059901 (2008).
[20] M. Glück, E. Reya, and A. Vogt, Eur. Phys. J. C **5**, 461 (1998), arXiv:hep-ph/9806404.
[21] A. Bodek and U. K. Yang, Nucl. Phys. B Proc. Suppl. **112**, 70 (2002), arXiv:hep-ex/0203009.
[22] T. Sjostrand, Computer Physics Communications **82**, 74 (1994).
[23] T. Sjostrand, S. Mrenna, and P. Z. Skands, JHEP **05**, 026 (2006), arXiv:hep-ph/0603175.
[24] T. Yang, C. Andreopoulos, H. Gallagher, K. Hoffmann, and P. Kehayias, Eur. Phys. J. C **63**, 1 (2009), arXiv:0904.4043 [hep-ph].
[25] J. Tena-Vidal *et al.* (GENIE), Phys. Rev. D **105**, 012009 (2022), arXiv:2106.05884 [hep-ph].
[26] A. Boudard, J. Cugnon, J.-C. David, S. Leray, and D. Mancusi, Phys. Rev. C **87**, 014606 (2013), arXiv:1210.3498 [nucl-th].
[27] A. Heikkinen, N. Stepanov, and J. P. Wellisch, eConf **C0303241**, MOMT008 (2003), arXiv:nucl-th/0306008.
[28] A. Ershova, S. Bolognesi, A. Letourneau, J.-C. David, S. Dolan, J. Hirtz, K. Niewczas, J. T. Sobczyk, A. Blanchet, M. B. Avanzini, *et al.*, Physical Review D **106**, 032009 (2022).
[29] C. Wilkinson, S. Dolan, L. Pickering, and C. Wret, Eur. Phys. J. C **82**, 808 (2022), arXiv:2203.11821 [hep-ph].
[30] A. Abed Abud *et al.* (DUNE), Instruments **5**, 31 (2021), arXiv:2103.13910 [physics.ins-det].
[31] X. G. Lu, L. Pickering, S. Dolan, G. Barr, D. Coplowe, Y. Uchida, D. Wark, M. O. Wascko, A. Weber, and T. Yuan, Phys. Rev. C **94**, 015503 (2016), arXiv:1512.05748 [nucl-th].
[32] X. G. Lu, D. Coplowe, R. Shah, G. Barr, D. Wark, and A. Weber, Phys. Rev. D **92**, 051302 (2015), arXiv:1507.00967 [hep-ex].
[33] A. P. Furmanski and J. T. Sobczyk, Phys. Rev. C **95**, 065501 (2017), arXiv:1609.03530 [hep-ex].
[34] P. Abratenko *et al.* (MicroBooNE), Phys. Rev. D **109**, 092007 (2024), arXiv:2310.06082 [nucl-ex].
[35] A. Abed Abud *et al.* (DUNE), JINST **19**, P12005 (2024), arXiv:2408.12725 [physics.ins-det].
[36] R. Acciarri *et al.* (LArIAT), JINST **15**, P04026 (2020), arXiv:1911.10379 [physics.ins-det].
[37] B. Abi *et al.* (DUNE), (2017), arXiv:1706.07081 [physics.ins-det].
[38] B. Abi *et al.* (DUNE), JINST **15**, P12004 (2020), arXiv:2007.06722 [physics.ins-det].
[39] E. Gramellini *et al.* (LArIAT), Phys. Rev. D **106**, 052009 (2022), arXiv:2108.00040 [hep-ex].
[40] A. Abed Abud *et al.* (DUNE), Phys. Rev. D **110**, 092011 (2024), arXiv:2408.00582 [hep-ex].
[41] F. Hojeij (HADES), PoS **FAIRness2022**, 023 (2023).
[42] B. Ramstein (HADES), EPJ Web Conf. **291**, 04004 (2024).
[43] R. Acciarri *et al.* (MicroBooNE), JINST **12**, P02017 (2017), arXiv:1612.05824 [physics.ins-det].
[44] P. A. Machado, O. Palamara, and D. W. Schmitz, Ann. Rev. Nucl. Part. Sci. **69**, 363 (2019), arXiv:1903.04608 [hep-ex].
[45] S. Amerio *et al.* (ICARUS), Nucl. Instrum. Meth. A **527**, 329 (2004).
[46] S. Abbaslu *et al.* (DUNE), (2025), arXiv:2509.07012 [physics.ins-det].
[47] A. M. Ankowski *et al.*, J. Phys. G **50**, 120501 (2023), arXiv:2203.06853 [hep-ex].
[48] S. Dytman *et al.* (CLAS), (2025), arXiv:2508.01905 [hep-ex].
[49] F. Acerbi *et al.*, (2025), arXiv:2503.21589 [hep-ex].

SUPPLEMENTAL MATERIAL

In addition to the studies presented in the main text, we have tested the effect of FSI modeling on the measurement of the $\sin^2\theta_{23}$ parameter. This is illustrated in Figure 4, where comparisons of FSI model variations with $\pm 1.3\%$ variations of $\sin^2\theta_{23}$ (chosen to be indicative of the target precision of next-generation experiments) show that the former can be disambiguated from the latter. This is because changes in $\sin^2\theta_{23}$ mainly affect the normalization of the spectra in the region of the oscillation dip whilst variations of FSI tend to shift the distribution.

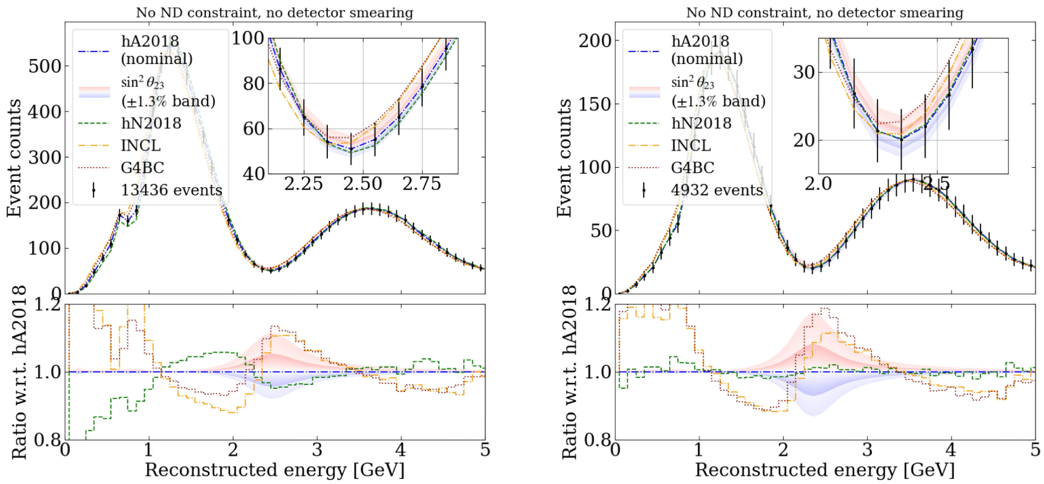

Fig. 4: Comparison of the simulated ν_μ reconstructed energy spectra and an oscillated DUNE experiment flux using different FSI models, to ±1.3% variations of $\sin^2\theta_{23}$. This is simulated for neutrino (top) and antineutrino (bottom) beam modes. Other figure elements follow the same conventions as described in Figure 2.